


RESEARCH

Open Access



Early upregulation of cytosolic phospholipase A₂α in motor neurons is induced by misfolded SOD1 in a mouse model of amyotrophic lateral sclerosis

Yafa Fetfet Malada Edelstein¹, Yulia Solomonov¹, Nurit Hadad¹, Leenor Alfahel², Adrian Israelson² and Rachel Levy^{1*} 

Abstract

Background: Amyotrophic lateral sclerosis (ALS) is a fatal multifactorial neurodegenerative disease characterized by the selective death of motor neurons. Cytosolic phospholipase A₂ alpha (cPLA₂α) upregulation and activation in the spinal cord of ALS patients has been reported. We have previously shown that cPLA₂α upregulation in the spinal cord of mutant SOD1 transgenic mice (SOD1^{G93A}) was detected long before the development of the disease, and inhibition of cPLA₂α upregulation delayed the disease's onset. The aim of the present study was to determine the mechanism for cPLA₂α upregulation.

Methods: Immunofluorescence analysis and western blot analysis of misfolded SOD1, cPLA₂α and inflammatory markers were performed in the spinal cord sections of SOD1^{G93A} transgenic mice and in primary motor neurons. Over expression of mutant SOD1 was performed by induction or transfection in primary motor neurons and in differentiated NSC34 motor neuron like cells.

Results: Misfolded SOD1 was detected in the spinal cord of 3 weeks old mutant SOD1^{G93A} mice before cPLA₂α upregulation. Elevated expression of both misfolded SOD1 and cPLA₂α was specifically detected in the motor neurons at 6 weeks with a high correlation between them. Elevated TNFα levels were detected in the spinal cord lysates of 6 weeks old mutant SOD1^{G93A} mice. Elevated TNFα was specifically detected in the motor neurons and its expression was highly correlated with cPLA₂α expression at 6 weeks. Induction of mutant SOD1 in primary motor neurons induced cPLA₂α and TNFα upregulation. Over expression of mutant SOD1 in NSC34 cells caused cPLA₂α upregulation which was prevented by antibodies against TNFα. The addition of TNFα to NSC34 cells caused cPLA₂α upregulation in a dose dependent manner.

Conclusions: Motor neurons expressing elevated cPLA₂α and TNFα are in an inflammatory state as early as at 6 weeks old mutant SOD1^{G93A} mice long before the development of the disease. Accumulated misfolded SOD1 in the motor neurons induced cPLA₂α upregulation via induction of TNFα.

*Correspondence: ral@bgu.ac.il

¹ Immunology and Infectious Diseases Laboratory, Department of Clinical Biochemistry and Pharmacology, Faculty of Health Sciences, Ben-Gurion University of the Negev and Soroka University Medical Center, 84105 Beer Sheva, Israel

Full list of author information is available at the end of the article



© The Author(s) 2021. **Open Access** This article is licensed under a Creative Commons Attribution 4.0 International License, which permits use, sharing, adaptation, distribution and reproduction in any medium or format, as long as you give appropriate credit to the original author(s) and the source, provide a link to the Creative Commons licence, and indicate if changes were made. The images or other third party material in this article are included in the article's Creative Commons licence, unless indicated otherwise in a credit line to the material. If material is not included in the article's Creative Commons licence and your intended use is not permitted by statutory regulation or exceeds the permitted use, you will need to obtain permission directly from the copyright holder. To view a copy of this licence, visit <http://creativecommons.org/licenses/by/4.0/>. The Creative Commons Public Domain Dedication waiver (<http://creativecommons.org/publicdomain/zero/1.0/>) applies to the data made available in this article, unless otherwise stated in a credit line to the data.

Keywords: Cytosolic phospholipase A₂α, ALS, Mutant SOD1^{G93A}, Motor neurons, TNFα, Misfolded SOD1

Background

Amyotrophic lateral sclerosis (ALS) is a severe degenerative disorder, mainly affecting the motor neurons. Most of the cases (about 90%) are sporadic. Familial cases have been linked to mutations in several genes, including chromosome 9 open reading frame 72 (C9ORF72) repeat expansions, Cu/Zn superoxide dismutase (SOD1), TAR DNA binding protein (TDP-43) and others [1]. Mutant SOD1 is the best characterized form of familial ALS, accounting for 20% of familial cases [2]. It is generally believed that sporadic and familial ALS may share pathological mechanisms. The pathophysiology of the multifactorial-multisystemic ALS disease includes various mechanisms. Although ALS is not primarily considered an inflammatory or immune-mediated disease, inflammation appears to play a role in the pathogenesis of the disease in both ALS patients and animal models, inflammatory responses have been observed [3–5]. Microglia [6] and astrocytes [7] are activated during the progression of the disease, and evidence suggests that they contribute to neuronal death.

Previous findings suggested that cytosolic phospholipase A₂α (cPLA₂α) is regarded as an essential source of inflammation. cPLA₂α specifically hydrolyzes phospholipids containing arachidonic acid at the sn-2 position [8, 9] and is the rate-limiting step in the generating eicosanoids and a platelet activating factor. These lipid mediators play critical roles in the initiation and modulation of inflammation and oxidative stress. cPLA₂α is ubiquitous in all cells and is essential for their physiological regulation. However, elevated cPLA₂α expression and activity were detected in the inflammatory sites in a vast array of inflammatory diseases, including neurodegenerative diseases [10–12]. Increased expression and activity of cPLA₂α has been detected in neurons, astrocytes and microglia in the spinal cord, brainstem and cortex of sporadic ALS patients [13] and in the spinal cord of mutant SOD1^{G93A} transgenic mice [14], suggesting that cPLA₂α may have an important role in the pathogenesis of the disease in all ALS patients. Our previous study [15] demonstrated that cPLA₂α is upregulated in the spinal cord of 6 weeks old SOD1^{G93A} mice long before the appearance of the disease symptoms, neuronal death or gliosis, and remained elevated during the whole life span of the mice. Prevention of cPLA₂α upregulation shortly before the onset of the disease symptoms, significantly delayed the loss of motor neuronal function, suggesting that cPLA₂α upregulation in the spinal cord plays a role in the disease pathology. The mechanism that induces

cPLA₂α elevation in the spinal cord of as early as 6 weeks old mice, is not yet clear. SOD1 insoluble protein complexes (IPCs) were detected in motor neurons of 30 days old SOD1^{G93A} mice [16], before the manifestation of ALS pathology, and several months before the appearance of inclusion bodies. The present study aims to determine whether accumulated misfolded SOD1 triggers cPLA₂α upregulation in motor neurons in the spinal cord of 6 weeks old ALS mice.

Methods

Animals

B6.Cg-Tg(SOD1G93A)1Gur/J hemizygous transgenic male mice were obtained from Jackson Laboratory (Bar Harbor, ME, U.S.A). The hemizygous transgenic male mice were also obtained by mating hemizygous transgenic males with C57BL/6J females (Jackson Laboratory). Each litter would generate hemizygous SOD1^{G93A} transgenic mice and littermate wild type controls as done before [15]. Transgenic male offspring were genotyped by PCR assay of DNA obtained from tail tissue (according to Jackson Laboratory). The study included male mice to avoid the estrogen effect. The study was approved by Ben-Gurion University Institutional Animal Care and Use Committee (IL-40-07-2016) and was conducted according to the Israeli Animal Welfare Act following the Guide for Care and Use of Laboratory Animal (National Research Council, 1996).

Motor function measurement by Rotarod A Rotarod test was used to evaluate the motor performance of the mice using an accelerating paradigm of 0.12 rpm/s as described before [15]. After a learning period of several days, mice were able to stay on the Rotarod (Rotamex-5, Columbus instruments, Columbus, OH, USA) for up to 150 s. Each mouse was given 3 trials and the best performance was used as a measure for motor function ability. Mice were tested twice a week from age of the 7 weeks-old until they could no longer perform the task.

Spinal cord tissue preparation Mice were deeply anesthetized and transcardially perfused with 20 ml of PBS [17].

For immunoblot analysis or immunoprecipitation Spinal cords were harvested in Lysis buffer containing 20 mM Tris pH7.5, 150 mM NaCl, 0.5% Sodium deoxycholate, 0.1% SDS, 0.1% Triton, 1 mM Phenylmethylsulfonyl fluoride and 1% protease inhibitors (Roche, Mannheim, Germany). The suspensions were sonicated 3 times for 20 s with Microsom Heatsystem Sonicator and centrifugated at 13,000×g for 20 min at 4 °C.

Immunoprecipitation of cPLA₂α or misfolded SOD1 was performed as described earlier [18, 19]. Spinal cords (100 μg) were solubilized in IP buffer (50 mM Tris–HCl pH 7.4, 150 mM NaCl, 1 mM EDTA, 0.5% Nonidet P-40, plus 1 × protease inhibitors) and incubated overnight with B8H10 antibodies (MédiMabs) or cPLA₂α antibodies previously cross-linked to magnetic beads (Invitrogen, Waltham, Massachusetts, USA) with dimethyl pimelimidate (Pierce) according to the manufacturer's instructions. The beads were magnetically isolated and washed three times with IP buffer. Samples were eluted by boiling in a 2 × SDS sample buffer. Lysate protein or resolved proteins were separated on 7% or 15% SDS-PAGE electrophoresis and transferred to nitrocellulose or PVDF membranes. Membranes were incubated in Tris-buffered saline (10 mM Tris, 135 mM NaCl, pH 7.4), with 0.1% Tween 20 (TBS-T) containing 5% non-fat milk for 1.5 h at 25 °C. The blots were then incubated with primary antibodies: 1:1000 rabbit anti-cPLA₂ (Cell Signaling Danvers, MA USA), 1:250 mouse B8H10 anti-misfolded human SOD1 (Medimabs, Quebec, Canada), 1:1000 rabbit anti-calreticulin (Thermo Scientific, IL, USA) as primary antibodies for overnight at 4 °C. After washing with TBS-T, they were incubated with secondary antibody: peroxidase conjugated goat anti-rabbit or anti mouse (Amersham Biosciences, Buckinghamshire, United Kingdom) for 1 h at 25 °C and developed using the enhanced chemiluminescence (ECL) detection system (PerkinElmer, Waltham, MA, USA). Proteins were quantified using video densitometry analysis (ImageJ version 4.0 Fuji).

For immunostaining—The spinal cords were fixed [15] in paraformaldehyde 4%/PBS solution overnight at 4 °C. The spinal cords were then transferred to PBS containing 30% sucrose for 24 h and then embedded in a 1:2 mixture of 30% sucrose in PBS:Tissue-Tek OCT (VWR, Radnor, PA), frozen in liquid nitrogen and stored at – 80 °C. Sections were made by cryostat (Leica Biosystems, Vienna, Austria) at 12 μm thickness, washed in PBS/tween 0.05%, incubated in PBS/Glycine 0.1% for 5 min and incubated in blocking solution (3% normal donkey serum and 2% BSA) at room temperature for 1 h. Then, these sections were incubated with primary antibodies diluted in blocking solution overnight at 4 °C. The primary antibodies used in the study were: 1:100 rabbit anti-cPLA₂ (Santa Cruz Biotechnology, Santa Cruz, CA, USA), rabbit anti-pcPLA₂α (Cell Signaling Danvers, MA USA), 1:100 mouse anti-misfolded human SOD1 (Medimabs, Quebec, Canada), 1:100 mouse anti-TNFα (Novus Biological USA, CO, USA), 1:100 goat anti-choline Acetyl-transferase (ChAT) (Millipore, CA, USA), 1:1000 rabbit anti-Iba-1 (Wako Pure Chemical Industries, Osaka, Japan), 1:500 rabbit anti-GFAP (Dako Glostrup

Denmark), 1:100 mouse anti-GFAP (Millipore Darmstadt, Germany). Sections were washed with PBS/tween 0.05%, and incubated with 1:200 Cy3 or 1:100 anti-mouse Alexa488 or anti-rabbit Dylight conjugated secondary antibodies (Jackson ImmunoResearch Laboratories, West Grove, PA, USA) for 1 h at room temperature. The staining of samples from the different treatments was performed in parallel. For each treatment, a negative control was prepared by omitting the primary antibody. Sections were mounted with anti-fading mounting medium (Electron Microscopy Sciences (EMS), Hatfield, PA, USA) and photographed in a blinded fashion using a fluorescent microscope (Olympus, BX60, Hamburg, Germany) or with confocal microscopy (Olympus, FluoView 1000, Tokyo, Japan). Using a confocal microscope, Z-sections were taken at 0.5 μm intervals and the results present Z-stack images. Fluorescence intensity was determined for cPLA₂α using CellProfiler program. The % of fluorescence intensity of cell area was determined for the different cell types using CellProfiler program. LSM880 inverted laser-scanning confocal microscope (Zena, Germany) equipped with an Airyscan high-resolution detection unit and under identical acquisition conditions was also used. A Plain-Apochromat 63x/1.4 Oil DIC M27 objective was used, and parameters were set to avoid pixel intensity saturation and to ensure Nyquist sampling in the XY plane. Excitation of lasers for DAPI, Alexa 488 and Cy3 were 405 nm, 488 nm and 561 nm, respectively.

Cell cultures

A Motor neurons were isolated as described before with few modifications. Briefly, spinal cords were dissociated from C57BL/6J mouse embryos at day 13.5 (E13.5) with 2 mg/ml papain for 25 min at 37 °C, and triturated with 0.5% bovine serum albumin (BSA) and 0.01 mg/ml DNase I in Leibovitz's L-15 medium (Gibco). Cells were then triturated with Leibovitz's L-15 media and the single-cells suspension was separated through Optiprep gradient (Sigma) and seeded at a density of 50,000 cells/24 well on coverslips pre-covered polyornithine (Sigma) and laminin (Sigma). The motor neurons were cultured with Neurobasal media (Gibco) supplemented with B27 (Gibco), 2% horse serum (Sigma), 1 ng/ml CNTF (R&D systems), and 1 ng/ml GDNF (R&D systems) and maintained at 37 °C in a 5% CO₂ humidified incubator. At 6 DIV, glial cells were inhibited using 5-Fluoro-2'-deoxyuridine (Sigma) and uridine (Sigma). For expression of human SOD1 in motor neurons, the cells were infected at 7 DIV using AAV1/2-SOD1^{WT} or AAV1/2-SOD1^{G93A} as previously described [20].

B Motor neuron like NSC34 cell line—were maintained in Dulbecco's modified Eagle's medium (DMEM) supplemented with 10% fetal calf serum (FCS) and 1%

penicillin/streptomycin solution at 37 °C with 5% CO₂ and were sub-cultured every 2–3 days [21]. For differentiation, the proliferation medium (DMEM, 10% FCS, 1% P/S) was exchanged 24 h after seeding with a differentiation medium containing 1:1 DMEM/F-12 (Ham), 1% FCS, 1% modified Eagle's medium nonessential amino acids (NEAA), 1% P/S and 1 μM all- trans retinoic acid. SOD1^{WT} and SOD1^{G93A} were constructed and purified as described before [22]. Transfection was performed by using TurboFect (Thermo) according to the manufacturer's protocol. TNF-α-neutralizing antibody (Cell Signaling Technology, Danvers, MA, USA) was used to study its effect.

Cell lysates—were prepared using lysis buffer containing: 2% Triton X-100, 50 mM HEPES (pH 7.5), 150 mM NaCl, 1 mM EDTA, 1 mM EGTA, 10% glycerol, 10 μM MgCl₂, 10 μg/ml leupeptin, 1 mM phenyl-methylsulphonylfluoride, 10 μg/ml aprotinin, 1 mM benzamidine, 20 mM para-nitrophenyl phosphate, 5 mM sodium orthovanadate, 10 mM sodium fluoride, and 50 mM β-glycerophosphate. Cell lysates were analyzed by SDS-PAGE on 15–10% gels. The amount of protein in each sample was quantified with the Pierce BCA Proteins Assay using BSA standards. The resolved proteins were transferred to PVDF membrane and blocked in 5% BSA in TBS-T (10 mM Tris, 135 mM NaCl, pH 7.4, 0.1% Tween 20). The detection of immunoreactive bands was carried out as described above but for cPLA₂α, using 1:500 rabbit anti cPLA₂α (GeneTex Inc, Alton Pkwy Irvine, CA, USA).

TNFα levels—were measured by a TNFα high sensitivity ELISA, eBioscience, Vienna, Austria.

Statistical analysis

Data were expressed as mean ± standard error of the mean (SEM). Statistical significance was determined by

either one- or two-way analysis of variance (ANOVA) followed by a posteriori Bonferroni's test for multiple comparisons provided by GraphPad Prism version 5.00 for Windows (GraphPad Software, San Diego, CA, USA). Pearson coefficient correlation (*r*) was used to study the relationships between the variables.

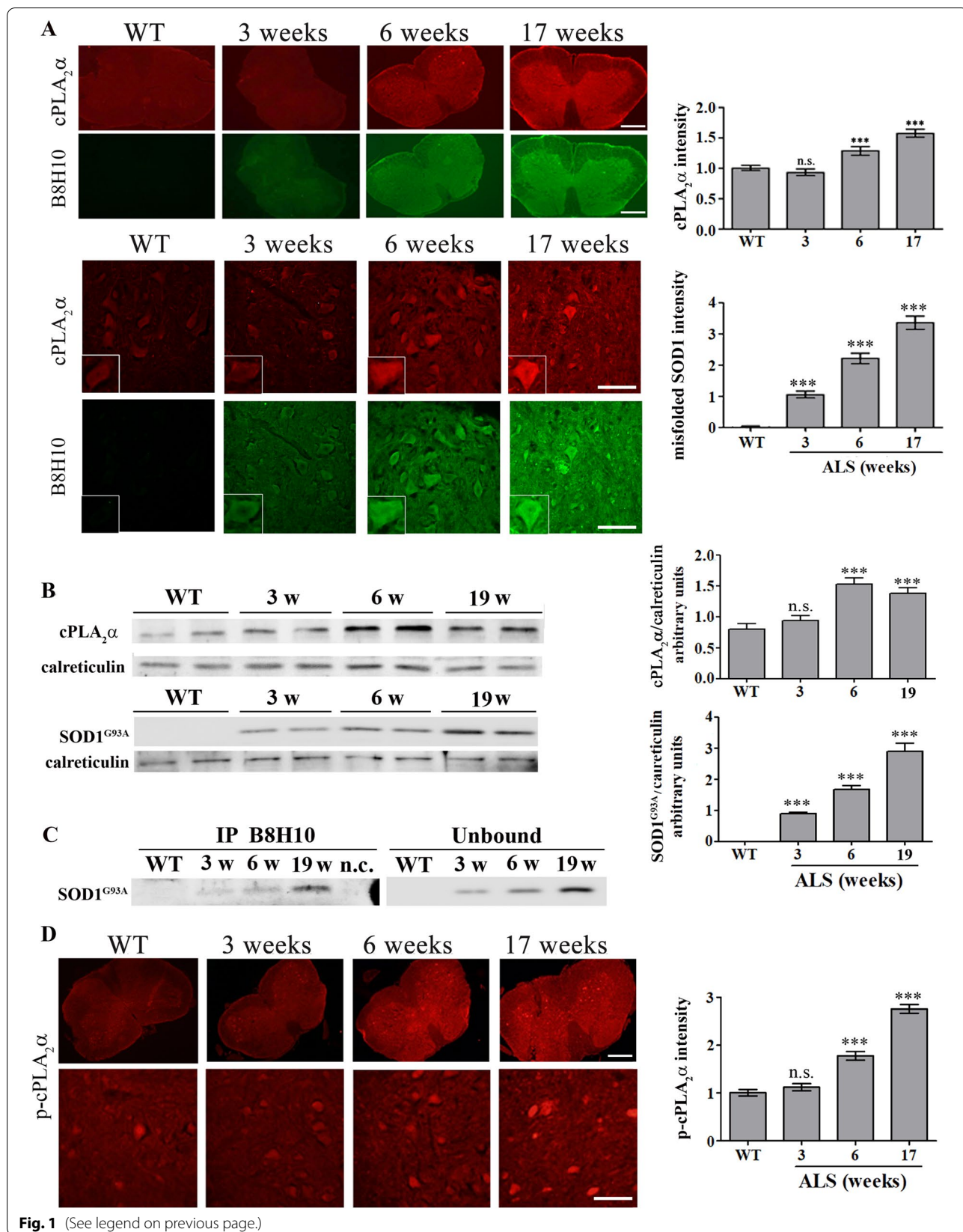
Results

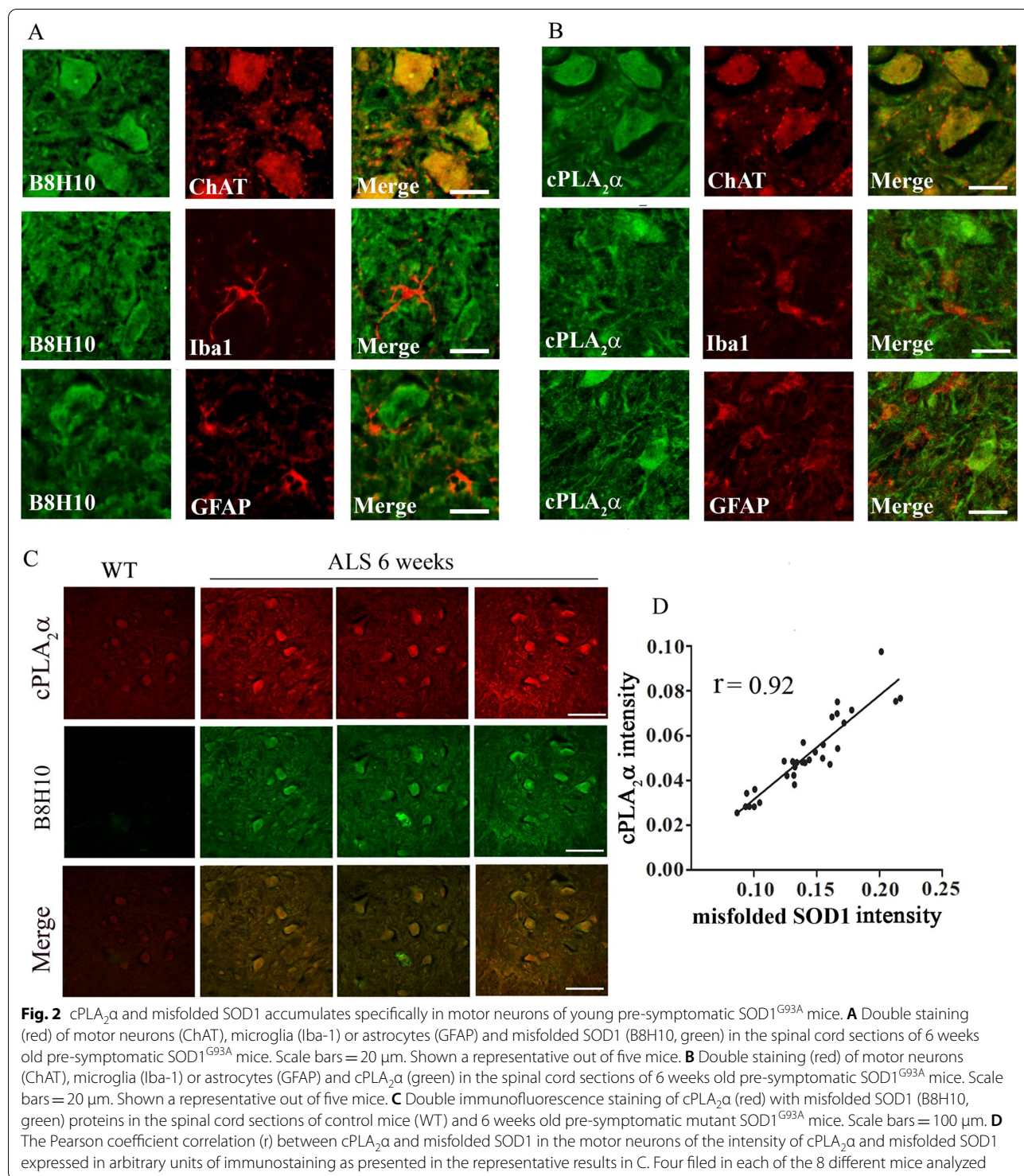
In our previous study we reported that cPLA₂α is elevated in the spinal cord of 6 weeks old mutant SOD1^{G93A} mice but not at 3 weeks. To study whether cPLA₂α is affected by the accumulation of misfolded SOD1 in the cells, cPLA₂α and misfolded SOD1 proteins expression and accumulation were analyzed in the spinal cord of SOD1^{G93A} mice. Immunofluorescence staining and quantitation showed a significant (*p* < 0.001) elevation of cPLA₂α protein expression in the spinal cord sections (Fig. 1A) of 6 weeks old SOD1^{G93A} mice, as shown in our previous study [15]. Immunofluorescence staining and quantitation of misfolded SOD1 showed that it was significantly (*p* < 0.001) detected in the spinal cord at 3 weeks old SOD1^{G93A} mice, before the elevation of cPLA₂α. The expression of cPLA₂α and mutant SOD1^{G93A} was also determined by western blot analysis and showed that mutant SOD1^{G93A} was detected at 3 weeks preceding the elevation of cPLA₂α (Fig. 1B). Moreover, misfolded SOD1 determined by immunoprecipitation with anti B8H10 was detected at 3 weeks in the spinal cord of SOD1^{G93A} mice and gradually increased at a later age (Fig. 1C). Activation of cPLA₂α analyzed by immunostaining of phosphor- cPLA₂α was detected at the spinal cord section of 6 weeks old SOD1^{G93A} mice but not at 3 weeks (Fig. 1D).

The elevated accumulation of misfolded SOD1 and the elevated cPLA₂α protein expression in the spinal cord sections of 6 weeks old mutant SOD1^{G93A} mice were

(See figure on next page.)

Fig. 1 Misfolded SOD1 accumulation precedes cPLA₂α upregulation and activation. **A** A representative double immunofluorescence staining of cPLA₂α (red) and misfolded SOD1 (B8H10, green) proteins in the lumbar spinal cord sections of WT and mutant SOD1^{G93A} mice during the development of the disease (3, 6 and 17 weeks). Scale bars = 500 μm (upper panel), 100 μm (lower panel) and inset 20 μm. The means ± SEM fluorescence intensity for both magnifications are presented in the bar graph as arbitrary units. Four mice for each time point and five fields for each mouse were analyzed. ****p* < 0.001 compared to control mice (WT). n.s. non-significant. **B** A representative immunoblot analysis of cPLA₂α, mutant SOD1^{G93A} and their corresponding calreticulin protein expression in the spinal cord lysates of WT and mutant SOD1^{G93A} mice during the development of the disease. cPLA₂α protein expression was determined by dividing the intensity of each cPLA₂α or mutant SOD1^{G93A} (SOD1^{G93A}) by the intensity of the corresponding calreticulin band after quantitation by densitometry and expressed in the bar graph as arbitrary units. The bar graphs are the means ± SE of 4 mice in each group. ****p* < 0.001 significance—compared to control mice (WT). n.s. non-significant. **C** Misfolded SOD1 was immunoprecipitated using anti-B8H10 antibodies from spinal cord lysates of WT and mutant SOD1^{G93A} mice during the development of the disease. A representative immunoblot analysis of the misfolded SOD1 (IP B8H10, left) and 10% of the unbound (Unbound, right) fractions are shown. nc- negative control, immunoprecipitation without anti-B8H10 antibodies. **D** A representative immunofluorescence staining of phosphor-cPLA₂α (p-cPLA₂α) in the lumbar spinal cord sections of WT and mutant SOD1^{G93A} mice during the development of the disease (3, 6 and 17 weeks). Scale bars = 500 μm (upper panel) and 100 μm (lower panel). The means ± SEM fluorescence intensity for both magnifications are presented in the bar graph in arbitrary units. Four mice for each time point and five fields for each mouse were analyzed. ****p* < 0.001 significance compared to WT mice. n.s. non-significant





detected specifically in motor neurons as determined by co-immunofluorescence staining of misfolded SOD1 and the marker of motor neurons ChAT (Fig. 2A). Using specific antibodies against misfolded SOD1 showed that elevated misfolded SOD1 was already detected at

3 weeks (Additional file 1: Fig. S1), and co-staining with ChAT showed that it is expressed in the motor neurons (Additional file 2: Fig. S2). Co-immunofluorescence staining of misfolded SOD1 and Iba1 or GFAP, the markers of microglia or astrocytes, respectively, showed that

misfolded SOD1 is not accumulated in these cells at 6 weeks (Fig. 2A). As shown by co-immunofluorescence staining, elevated cPLA₂α expression was also detected specifically in the motor neurons and not in microglia or astrocytes (Fig. 2B). Co-immunostaining of cPLA₂α and misfolded SOD1 showed co-localization and overlapping between cPLA₂α and misfolded SOD1 in the motor neurons in the spinal cord of 6 weeks old mutant SOD1^{G93A} mice (Fig. 2C). cPLA₂α upregulation showed some variation that highly correlated with the accumulation of misfolded SOD1 with a correlation coefficient of 0.92 between both proteins, suggesting that the level of misfolded SOD1 in the motor neurons defines the level of cPLA₂α protein expression (Fig. 2D). To determine whether the accumulation of misfolded SOD1 in the motor neurons is responsible for cPLA₂α upregulation, human SOD1^{WT} or mutant SOD1^{G93A} were expressed in primary motor neurons isolated from the spinal cord from C57BL/6J mouse embryos as shown in the western blot analysis (Fig. 3A). The expression of human SOD1 did not affect the morphology of the motor neurons and their number (Fig. 3B). Double staining with anti-B8H10 and anti-cPLA₂α showed elevated cPLA₂α protein expression in motor neurons expressing mutant SOD1^{G93A} and accumulating misfolded SOD1 (Fig. 3C). In motor neurons that did not accumulate misfolded SOD1 (as shown in Fig. 3A), cPLA₂α expression did not change and was similar to that detected in control motor neurons (without induction). These results clearly indicate that misfolded SOD1 induced cPLA₂α upregulation.

To study whether the elevated cPLA₂α protein expression is triggered or stabilized by an interaction between misfolded SOD1 and cPLA₂α, the binding between both proteins was determined by co-immunoprecipitation experiments. As shown in Fig. 4A, immunoprecipitation of cPLA₂α in the spinal cord lysates at disease onset (13 weeks), symptomatic stage (18 weeks) or end stage (Fig. 4B) resulted in a significant co-immunoprecipitation of mutant SOD1^{G93A} (Fig. 4A), suggesting a binding between them. In contrast, there was no co-immunoprecipitation of mutant SOD1^{G93A} and cPLA₂α in the spinal cord lysates of 6 weeks old mutant SOD1^{G93A} mice, suggesting that there is no binding between the proteins in

that early stage. We then used an Airyscan detector, a sub-diffraction high-resolution laser-scanning confocal microscope to examine the binding between both proteins. The Airyscan detector used in the current study provides improved lateral resolution (~150 nm) and signal to noise ratio, as compared with conventional confocal microscopes. Under these conditions, accurate and straight forward analysis of the interaction between misfolded SOD1 and cPLA₂α in the motor neurons in the spinal cord section was allowed. Airyscan high-resolution detection showed that there is only partial overlapping indicating partial binding between both proteins at 6 weeks (Fig. 4C, D).

Proinflammatory cytokines such as TNFα [23, 24] are shown to induce elevation of cPLA₂α protein expression, thus, we examined whether increased levels of TNFα could be detected in the spinal cord of 6 weeks old mutant SOD1^{G93A} mice. As shown in Fig. 5A, there is a significant ($p < 0.001$) elevation of TNFα in the spinal cord lysates of 6 weeks old mutant SOD1^{G93A} mice in comparison with spinal cord lysates of WT or 3 weeks old SOD1^{G93A} mice (130.0 ± 3.0 pg/ml compared with 85.5 ± 13.3 and 73.6 ± 6.7 pg/ml, respectively). To determine which type of cell produces TNFα, co-immunofluorescence staining of TNFα using anti-TNFα antibodies that show specific staining (Additional file 3: Fig. S3) and the different cell markers was performed in the spinal cord sections of 6 weeks old SOD1^{G93A} mice. Co-immunofluorescence staining of TNFα and ChAT clearly showed that TNFα was detected in the motor neurons in the spinal cords of 6 weeks old mutant SOD1^{G93A} mice (Fig. 5B). Immunofluorescence staining of the motor neurons in the spinal cord of 6 weeks old SOD1^{G93A} mice showed elevation of both TNFα receptors expression in comparison to WT mice (Additional file 4: Fig. S4). Co-immunofluorescence staining of TNFα and either Iba1 or GFAP showed that TNFα was not detected in the microglia or astrocytes at 6 weeks (Fig. 5B). A time course of co-immunofluorescence staining of TNFα and the different cell markers in the spinal cords of SOD1^{G93A} mice clearly shows elevated TNFα levels in the motor neurons at 6 weeks which was gradually increased at a later stage (Fig. 5C). TNFα was not detected in glia cells at 6 weeks,

(See figure on next page.)

Fig. 3 Accumulation of misfolded SOD1 in primary motor neurons induced cPLA₂α upregulation. **A** Immunoblot analysis of human SOD1^{WT} or mutant SOD1^{G93A} (hSOD1), expressed in primary motor neurons by infection of AAV1/2 as described in materials and methods. Immunoblot analysis of mouse SOD1 (mSOD1) is shown as a control. **B** Light microscope pictures of primary motor neurons. Control—without infection, motor neurons expressing human wild type SOD1 (SOD1 WT) or mutant SOD1 (SOD1 G93A). Scale bars = 50 μm. **C** Double immunofluorescence staining of cPLA₂α (green) with misfolded SOD1 (B8H10, red) in motor neurons expressing SOD1^{WT}, mutant SOD1^{G93A} and control cells. Two upper panels scale bars = 50 μm and two lower panels scale bars = 20 μm. 3 different independent experiments were analyzed and showed similar results. The means ± SEM fluorescence intensity for cPLA₂α and misfolded SOD1 is presented in the bar graphs as arbitrary units. Five fields in each of the 3 different treatments of motor neurons in each experiment was analyzed. Significance compared to control *** $p < 0.001$, n.s. non-significant

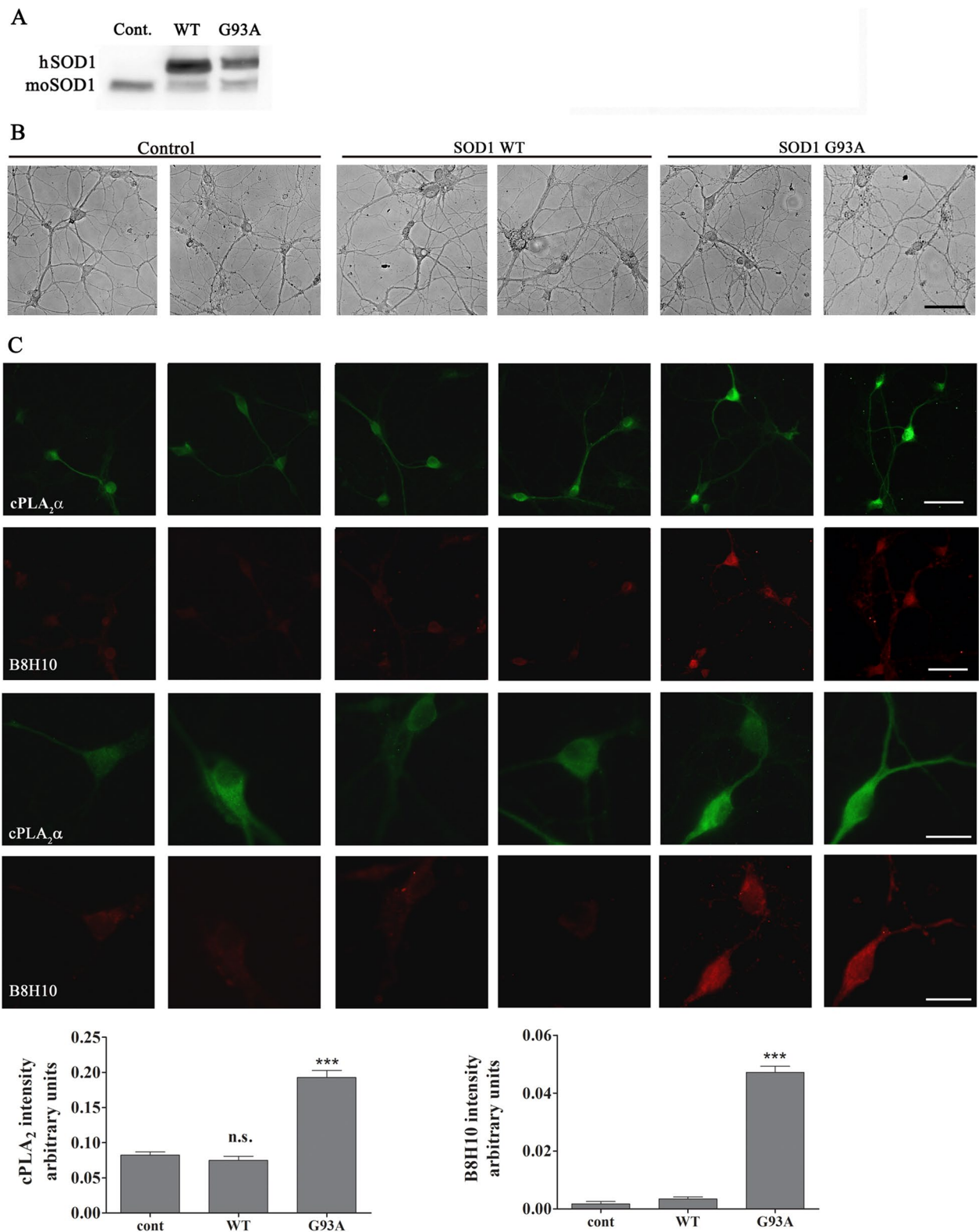


Fig. 3 (See legend on previous page.)

but was detected in microglia at 15 weeks and in astrocytes at 18 weeks (Fig. 5C). In accordance with these results, immunofluorescence staining of Iba1 or GFAP, to determine glia activation, showed no significant activation in the spinal cord section of mutant SOD1^{G93A} mice at these early stages (3 and 6 weeks), although misfolded SOD1 was already accumulated in the spinal cord, but did show a significant activation in the spinal cord sections of 17 weeks old SOD1^{G93A} mice (Additional file 5: Fig. S5) as reported in our previous study [15]. Co-immunofluorescence staining and densitometry analysis of cPLA₂α and TNFα in the spinal cord sections of 6 weeks old SOD1^{G93A} mice showed as above that there is a variation of elevated cPLA₂α protein expression in the different mice (Fig. 6A), which was highly correlated with TNFα (coefficient correlation, $r = 0.81$) in the motor neurons (Fig. 6B), suggesting that TNFα produced in the motor neurons is responsible for cPLA₂α upregulation. We next studied the effect of misfolded SOD1 accumulation on TNFα expression using motor neurons that were viral induced with human SOD1^{WT} or mutant SOD1^{G93A} (described in Fig. 3). As shown in Fig. 6C, double staining of cPLA₂α and TNFα showed that motor neurons with accumulated mutant SOD1^{G93A} (Fig. 3C) expressed elevated levels of both cPLA₂α and TNFα. Over expression of SOD1^{WT} did not affect cPLA₂α and TNFα compared with the control cells. The comparison between motor neurons expressing SOD1^{WT} and those expressing the mutant SOD1^{G93A} clearly shows that of the accumulation of misfolded SOD1 induces the elevation of cPLA₂α and TNFα (Additional file 6: Fig. S6). To determine whether elevated TNFα is responsible for cPLA₂α upregulation, human SOD1^{WT} or SOD1^{G93A} were expressed in the motor neurons like NSC34 cells. NSC34 is a hybrid cell line produced by the fusion of motor neurons from the spinal cords of mouse embryos with mouse neuroblastoma cells N18TG2 that exhibit properties of motor neurons after differentiation [21] as presented by shape change (Fig. 7A). As clearly shown in the western blot analysis (Fig. 7B), accumulation of mutant SOD1 caused significant elevation of cPLA₂α, while accumulation of SOD1^{WT} did not affect on cPLA₂α expression in NSC34 cells compared with the control (untransfected cells).

The presence of neutralizing TNFα antibodies (50 ng/ml) prevented cPLA₂α upregulation, indicating that TNFα is responsible for cPLA₂α upregulation by an autocrine mechanism. In accord with these results, although very low levels of TNFα were detected in the supernatant of the cells, they were significantly higher in supernatant of cells transfected with human SOD1^{G93A} compared with cells transfected with SOD1^{WT} or control cells (Additional file 7: Fig. S7). The differentiated neuron motors NSC34 cells express both TNF receptors as shown by immunofluorescence staining (Fig. 7C). The addition of TNFα to differentiated NSC34 cells caused cPLA₂α upregulation in a dose dependent manner, as shown by western blot analysis (Fig. 7D) and immunofluorescence staining cPLA₂α (Fig. 7E).

Discussion

The present study clearly demonstrates that misfolded SOD1 is significantly detected in the spinal cords of 3 weeks old mutant SOD1^{G93A} mice preceding the elevated expression of cPLA₂α and its activation at 6 weeks. The elevation of cPLA₂α in the spinal cords at 6 weeks, was detected specifically in motor neurons and not in microglia or astrocytes. While, at the symptomatic stage, elevated cPLA₂α was also detected in the glia cells in accordance with our and others previous studies [14, 15]. Similar to our results, activation and elevation of cPLA₂α protein expression were mainly detected in motor neurons in other pathological conditions such as after spinal cord injury and in spinal inflammatory hyperalgesia [25–29]. cPLA₂α is a major inflammatory enzyme-producing arachidonic acid, a substrate for the formation of eicosanoids and a platelet-activating factor which are well-known mediators of inflammation and tissue damage implicated in pathological states of several acute and chronic neurological disorders [26, 30–32]. The detection of elevated and activated cPLA₂α in the motor neurons at 6 weeks old mutant SOD1^{G93A} mice and long before any neuronal damage or sign of the disease is evident, indicates an inflammatory state of the motor neurons at this very early stage. Misfolded SOD1 accumulation in the spinal cord of 3 weeks old SOD1^{G93A} mice was detected in motor neurons but not in astrocytes or microglia.

(See figure on next page.)

Fig. 4 Partial binding between cPLA₂α and mutant SOD1^{G93A} in motor neurons of 6 weeks old mutant SOD1^{G93A} mice. **A** Immunoprecipitation with antibody against cPLA₂α and Western Blot analysis for cPLA₂α and mutant SOD1 in the spinal cord lysate of control (WT) and mutant SOD1^{G93A} mice during the development of the disease shown by a representative immunoblot. Negative control (n.c.) -without antibodies against cPLA₂α. **B** Motor performance on accelerating Rotarod test ($n = 10$ mice). The arrows show the immunoprecipitation analysis along the development of the disease. **C** Airyscan detector high resolution confocal microscopy images of double immunofluorescence staining of cPLA₂α (red) with misfolded SOD1 (B8H10, green) proteins in the spinal cord sections of 6 weeks old pre-symptomatic SOD1^{G93A} mouse. Scale bars = 20 μm. **D** The coupling of both proteins (cPLA₂α and misfolded SOD1) in the line shown by the arrow was analyzed and presented as intensity along the line. The ellipse shows an example of binding between both proteins

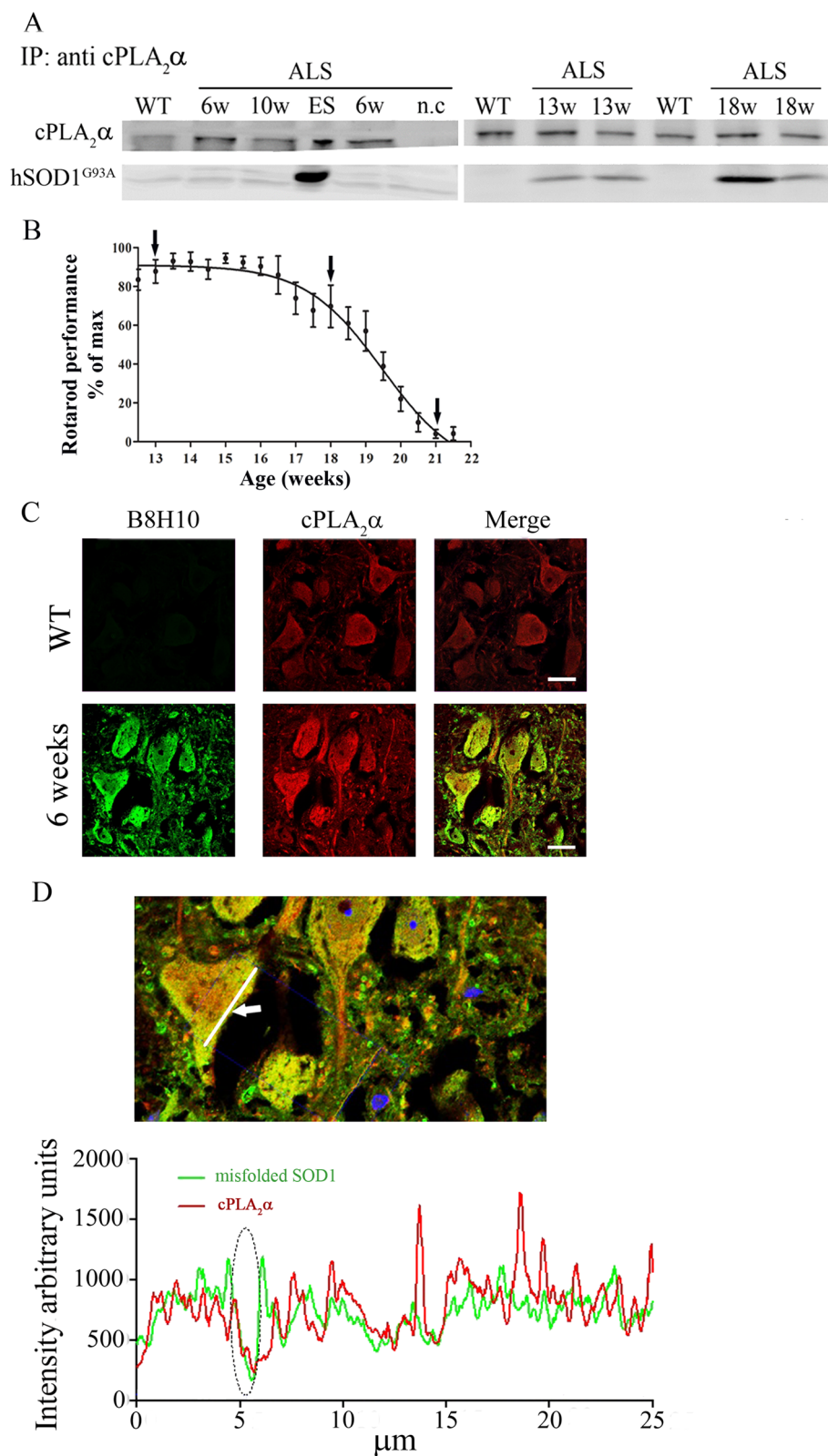


Fig. 4 (See legend on previous page.)

The significant accumulation of misfolded SOD1 in the motor neurons before the appearance of elevated cPLA₂α expression and the significant correlation ($r=0.92$) between both proteins at 6 weeks shown in the present study raised the possibility that the accumulation of misfolded SOD1 in the cells dictates the expression of cPLA₂α. Indeed, the accumulation of misfolded SOD1 (determined by B8H10 staining) in primary motor neurons isolated from the mouse spinal cord or expression of mutant SOD1 in NSC34 motor neuron-like cells caused a significant elevation of cPLA₂α protein expression. In contrast, expression of human SOD1^{WT} did not affect cPLA₂α expression, indicating that intracellular misfolded SOD1 induced cPLA₂α upregulation. Although the role of glial cells in neuronal damage and disease progression is well established [33], we show here that the elevation of cPLA₂α in the motor neurons at 6 weeks is independent of glia cells and occurs long before any neuronal damage. In accordance with our results, the effect of accumulated mutant SOD1 on cPLA₂α in NSC34 cells was reported recently [34]. They showed that expression of SOD1^{G93A} in motor neuron cell line NSC34 for long time induced cell death mediated by cPLA₂α. The elevated levels of cPLA₂α in familial and sporadic ALS [13] together with the observations that inclusions containing misfolded SOD1 are regularly present in motor neurons of ALS patients, both with and without SOD1 mutations [35], support the notion that misfolded SOD1 accumulated in the motor neurons contributes to the elevated cPLA₂α expression.

Induction or stabilization of proteins by other proteins within the cells via an interaction mechanism such as induction of P53 by elevated amyloid beta [36] and stabilization of EGFR or Kit C by HIP1 binding have been reported [37, 38]. In addition, binding and co-precipitation of oligomeric or misfolded SOD1 with other proteins including voltage dependent anion channel (VDAC1) [39, 40], macrophage migration inhibitory factor (MIF) [22, 41], heat shock protein [42], glutathione peroxidase 1 [43] or Bcl-2 [44] have been documented. Taken together, these observations and the results demonstrating high

overlapping of misfolded SOD1 and cPLA₂α in the motor neurons in spinal cord sections by confocal microscopy could suggest that cPLA₂α upregulation is induced by its interaction with misfolded SOD1 at 6 weeks old mutant SOD1^{G93A} mice. Co-immunoprecipitation of both proteins was detected only at the symptomatic stage but not at 6 weeks, indicating no direct interaction at this stage. Using the Airyscan detector, a sub-diffraction high-resolution laser-scanning confocal microscope [45, 46], we showed that only partial binding between both proteins in motor neurons at 6 weeks, explains the absence of co-immunoprecipitation at this stage, and questioning the possibility that the interaction between misfolded SOD1 and cPLA₂α induced the elevation of cPLA₂α expression.

cPLA₂α was shown to be induced by different pro-inflammatory mediators and insults through specific receptors or scavenger receptors [23, 47–50]. Ours and other studies reported that TNFα induced cPLA₂α upregulation in various systems [23, 51, 52] and in motor neuron-like NSC34 cells, as demonstrated in the present study. In the neural environment, constitutive physiological levels of TNFα regulate synaptic plasticity, modulates dendritic maturation, pruning, and synaptic connectivity to respond to alterations in sensory stimuli to maintain homeostatic plasticity [53, 54]. Overexpression of TNFα has been associated with neuronal excitotoxicity, synapse loss, and propagation of the inflammatory state [55]. TNFα elicits its wide range of biological responses by activating two distinct receptors, TNF-R1 and TNF-R2 [56–58]. Antigenic TNFα and its soluble receptors measured by ELISA were significantly higher in ALS patients than in healthy controls [59]. To our knowledge, the present study is the first to show a significant elevation of TNFα protein in the spinal cord of mutant SOD1^{G93A} mice as early as at 6 weeks, that was about 150% of the levels of TNFα in the spinal cord of WT mice and of 3 weeks old mutant SOD1^{G93A} mice. Our results are supported by other studies reporting that TNFα was detected in the spinal cord of late pre-symptomatic stage ALS mice. TNFα was the sole cytokine whose mRNA could be observed in the spinal cord of young

(See figure on next page.)

Fig. 5 Increased TNFα is restricted to the motor neurons of pre-symptomatic 6 weeks old mutant SOD1^{G93A} mice. **A** The levels of TNFα in the spinal cord lysate of WT and of 3 and 6 weeks old pre-symptomatic mutant SOD1^{G93A} mice detected by ELISA. Significance—*** $p < 0.001$, n.s. = non-significant. The bar graph is the mean \pm SE of 8 mice in each group. **B** Representative double immunofluorescence staining cell markers (green) of motor neurons (ChAT), microglia (Iba-1) or astrocytes (GFAP) and TNFα (red) in the spinal cord sections of 6 weeks old pre-symptomatic SOD1^{G93A} mice. Scale bars = 20 μ m. 3 other mice in each group were analyzed and showed similar results. **C** A representative time course of double immunofluorescence staining of TNFα (red) and cell markers (green) of motor neurons (ChAT), microglia (Iba-1) or astrocytes (GFAP) proteins in the lumbar spinal cord sections of WT and mutant SOD1^{G93A} mice during the course of the disease (3, 6, 15 and 18 weeks). Scale bars = 20 μ m. 3 other mice in each group were analyzed and showed similar results. **D** The means \pm SEM fluorescence intensity for TNFα is presented in the bar graph as arbitrary units. Four mice for each time point and five fields for each mouse were analyzed. Significance compared to control *** $p < 0.001$, n.s. non-significant

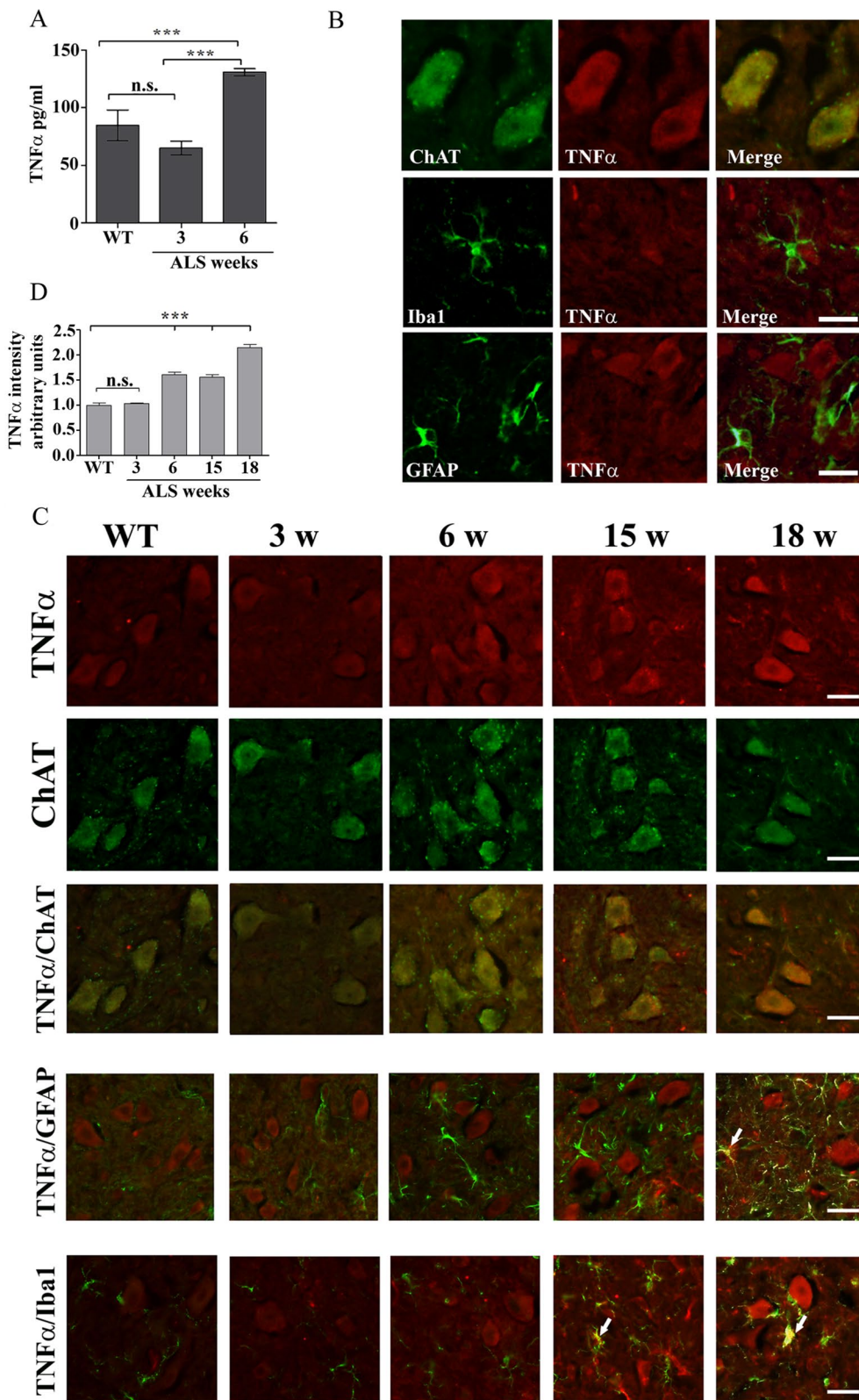


Fig. 5 (See legend on previous page.)

pre-symptomatic SOD1^{G93A} mice [60]. A microarray survey of 1081 gene products expressed in spinal cords of SOD1^{G93A} mice reported that TNF α was the only inflammatory cytokine found to be differentially expressed [4]. Upregulation of TNF α and its proapoptotic receptors mRNA were detected at late pre-symptomatic stages and preceded transcriptional upregulation of other pro-inflammatory gene products and temporally correlates with the progression of the disease in SOD1^{G93A} mice [61, 62]. TNF α was reported to be elevated in the spinal cord of SOD1^{G93A} transgenic mice in the early life span, at 80 days [63]. We also show here for the first time that elevated TNF α is expressed specifically in spinal motor neurons of 6 weeks old SOD1^{G93A} mice but not in microglia or astrocytes, although glia cells are reported to be the major cell type to secrete TNF α [64]. In agreement with our results, immunohistochemical analysis showed little TNF α immunoreactivity in motor neurons from 60 days old SOD1^{G93A} transgenic mice with a healthy appearance [65] and FasL as early as day 40 [65]. Since FasL is upregulated by TNF α [66], it is possible that due to the methodology sensitivity TNF α was not detected in the spinal cord of 40 days old SOD1^{G93A} mice but at 60 days in their study [65]. We show here a high correlation ($r=0.81$) between cPLA₂ α and TNF α expressed in the spinal motor neurons of 6 weeks old SOD1^{G93A} mice, suggesting that misfolded SOD1 induced the elevation of cPLA₂ α via production of TNF α . Indeed, as we show in the present study, that expression of mutant SOD1 but not SOD1^{WT} in motor neurons induced both cPLA₂ α and TNF α upregulation. Moreover, the presence of neutralizing TNF α antibodies prevented the elevation of cPLA₂ α expression NSC34 like motor neurons, indicating that TNF α is responsible for cPLA₂ α upregulation, acting via its autocrine effect. Likewise, addition of TNF α (10–100 pg/ml) to differentiated NSC34 cells for 24 h caused cPLA₂ α upregulation in a dose dependent manner similar to the concentration detected in the spinal cord of 6 weeks of SOD1^{G93A} mice. In agreement with our report, addition of soluble TNF α (acting through a reverse signaling) for 6 days affected motor neurons, inducing a marked motor neuron loss in SOD1-G93A

monocultures [33]. Since elevated TNF α receptors were detected in motor neurons in the spinal cord of 6 weeks old SOD1^{G93A} mice, in accordance with others that reported elevated TNFR in the pre-symptomatic stage [67], the elevated TNF α in the spinal cord at this time point probably acts through its receptors to induce cPLA₂ α upregulation.

Our results, suggesting that motor neurons have a crucial role in inflammatory state (demonstrating elevated both cPLA₂ α and TNF α) during the early stage of the disease, are in accordance with the specific activation of motor neurons but not glia cells in the pre-symptomatic stage (at 8 weeks) of the disease in mutant SOD1^{G93A} mice evident by the increased p38MAPK [67, 68], activation of ASK1, MKK3,4,6, overexpression of both TNF α receptors (TNFR1 and TNFR2) [67] and TNF α accumulation in transgenic motor neurons [33]. In addition, motor neurons were reported as a primary determinant of disease onset and early disease progression by selective mutant gene inactivation within the cells [69]. Moreover, it was shown [70] that neuronal expression of mutant SOD1 was sufficient to cause motor neuron degeneration and paralysis in transgenic mice with cytosolic dendritic ubiquitinated SOD1 aggregates as the dominant pathological feature. Crossing neuron-specific mutant SOD1 mice with ubiquitously wild-type SOD1-expressing mice led to dramatic wild-type SOD1 aggregation in oligodendroglia after the onset of neuronal degeneration suggesting that mutant SOD1 in neurons triggers neuronal degeneration, which in turn may facilitate aggregates formation in surrounding glial cells. In contrast, cell-specific deletion of mutant SOD1 in genetically altered mice has implicated microglia and astrocytes as contributors to the late disease progression but not the onset of disease [71–73].

Conclusions

We show here that elevated protein expression of both cPLA₂ α and TNF α were detected specifically in motor neurons and not in glial cells in the spinal cord of 6 weeks old SOD1^{G93A} mice, indicating the inflammatory state of the motor neurons long before the development of signs

(See figure on next page.)

Fig. 6 Elevated cPLA₂ α protein expression in the motor neurons is highly correlated with TNF α . **A** Double immunofluorescence staining of cPLA₂ α (green) and TNF α (red) proteins in the lumbar spinal cord sections of WT and 6 weeks old mutant SOD1^{G93A} mice. Scale bars = 100 μ m. **B** The Pearson coefficient correlation (r) between cPLA₂ α and TNF α in the spinal motor neurons of mutant SOD1^{G93A} mice was analyzed. Fluorescence intensity is expressed in arbitrary units of immunostaining as presented in the representative results in A. Four fields in each of the 8 different mice analyzed. **C** Elevated cPLA₂ α and TNF α in primary motor neurons expressing mutant SOD1^{G93A}. Double immunofluorescence staining of cPLA₂ α (green) and TNF α (red) in primary motor neurons expressing human SOD1^{WT}, mutant SOD1^{G93A} and control cells described in Fig. 3. Two upper panels, scale bars = 50 μ m and two lower panels, scale bars = 20 μ m. 3 different independent experiments were analyzed and showed similar results. The means \pm SEM fluorescence intensity for cPLA₂ α and TNF α is presented in the bar graphs as arbitrary units. Five fields in each of the 3 different treatments of motor neurons in each experiment was analyzed. Significance compared to control *** $p < 0.001$, n.s. non-significant

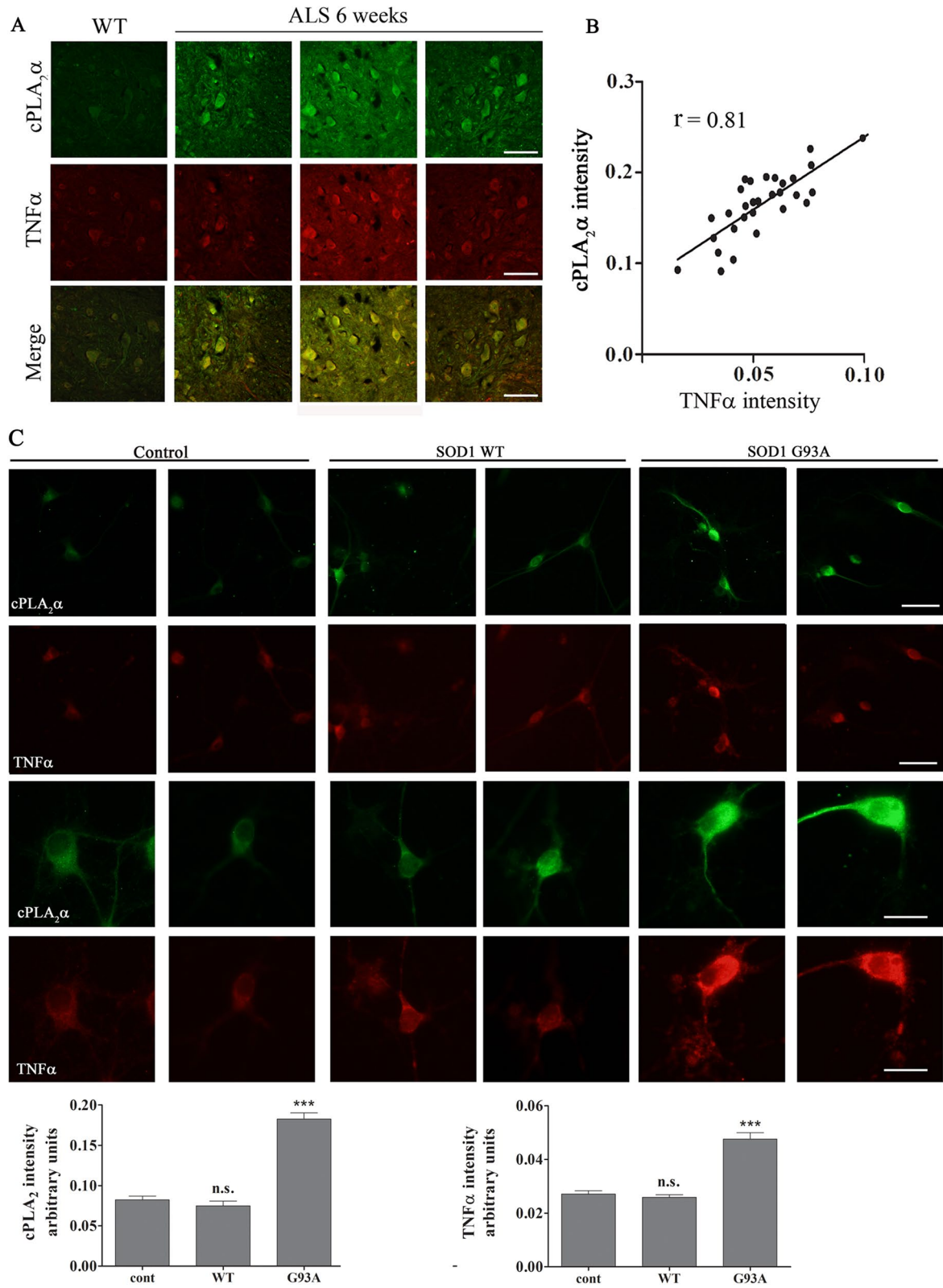
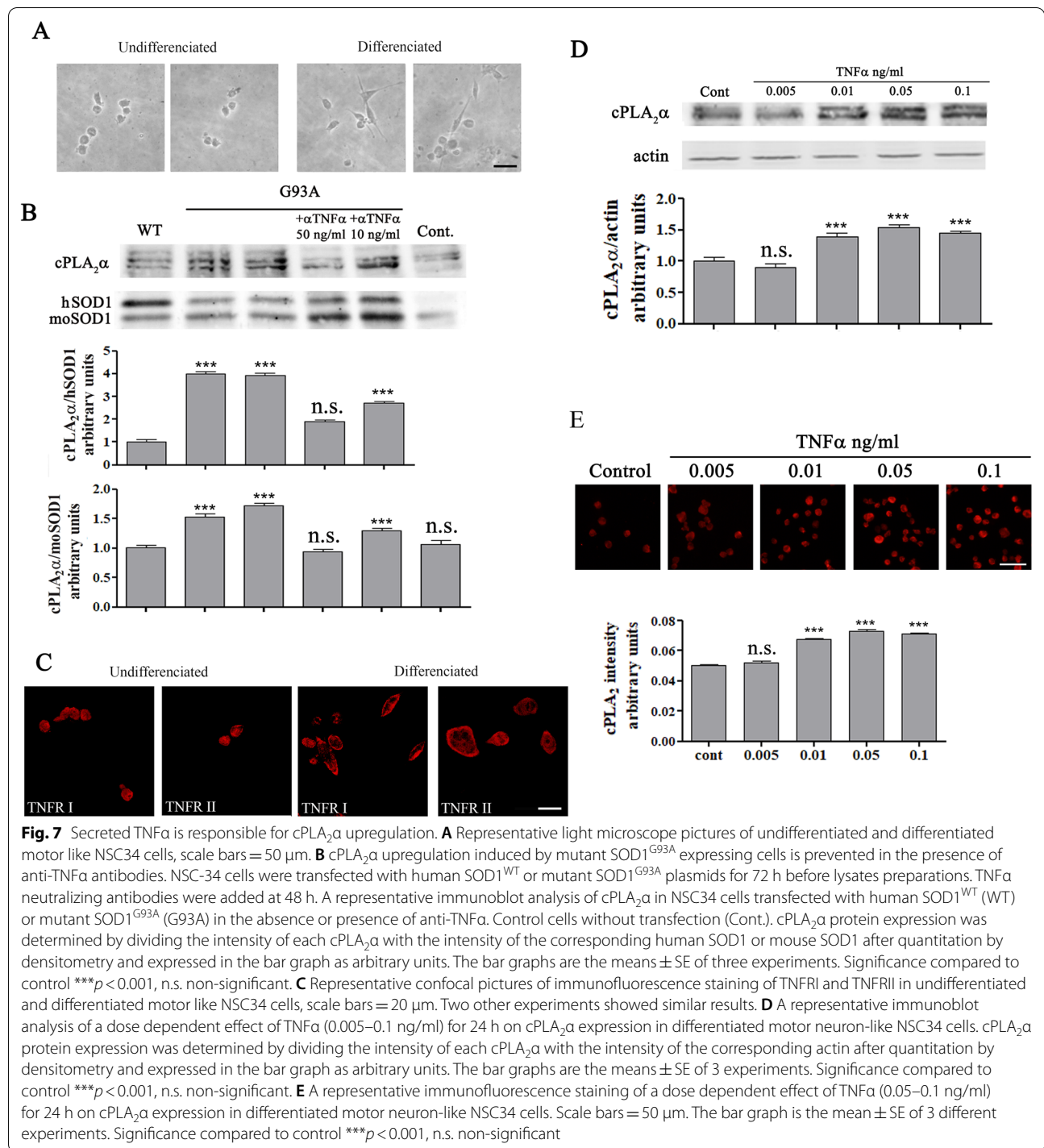


Fig. 6 (See legend on previous page.)



of the disease. Misfolded SOD1 is accumulated in the spinal cord motor neurons of 3 weeks old SOD1^{G93A} mice, preceding cPLA $_2\alpha$ and TNF α upregulation. The results of the present study show: **a.** The high correlation between cPLA $_2\alpha$ and misfolded SOD1 levels and between cPLA $_2\alpha$ and TNF α levels in the motor neurons at 6 weeks, **b.**

cPLA $_2\alpha$ and TNF α upregulation by expressing mutant SOD1 in primary motor neurons and in NSC34 motor neurons like cells, **c.** the prevention of cPLA $_2\alpha$ upregulation in the presence of TNF α neutralizing antibodies and **d.** the induction of cPLA $_2\alpha$ upregulation by addition of TNF α and the presence of TNFR receptors. Based on

these results we can conclude that accumulated misfolded SOD1, in the motor neurons in the spinal cord of 6 weeks old SOD1^{G93A} mice, induced cPLA₂α upregulation mediated by TNFα via its autocrine effect.

Abbreviations

ALS: Amyotrophic lateral sclerosis; cPLA₂α: Cytosolic phospholipase A2 alpha; SOD1^{G93A}: SOD1 transgenic mice; TNFα: Tumor necrosis factor alpha; hSOD1^{G93A}: Recombinant human mutant SOD1^{G93A}; WT: Wild type.

Supplementary Information

The online version contains supplementary material available at <https://doi.org/10.1186/s12974-021-02326-5>.

Additional file 1: Figure S1. Specificity of immunofluorescence analysis of misfolded SOD1. Representative results of immunofluorescence analysis of misfolded SOD1, using B8H10 antibodies, versus negative control (n.c.) and wild type (WT) in mice spinal cords. Scale bar = 100 μm.

Additional file 2: Figure S2. Misfolded SOD1 could be detected at 3 weeks in motor neurons. A representative double immunofluorescence of motor neurons marker (ChAT) and misfolded SOD1 in the spinal cord of 3 weeks old SOD1^{G93A} mice. Scale bar = 100 μm

Additional file 3: Figure S3. Specificity of immunofluorescence analysis of TNFα. Representative results of immunofluorescence staining of TNFα versus negative control (n.c.) in the spinal cord of WT mice and 6 weeks old SOD1^{G93A} mice. Scale bar = 100 μm. There is a low staining of TNFα in the spinal cord of WT mice in accordance with the low level of TNFα in their lysates.

Additional file 4: Figure S4. TNFα receptors are elevated in motor neurons in the spinal cord of 6 weeks old mutant SOD1^{G93A} mice. Representative immunofluorescence staining of TNFR1 and TNFR2 in the spinal cord of WT mice and mutant SOD1^{G93A} mice. Scale bars = 50 μm. The elevated receptors are detected in motor neurons as determined by the cell shape.

Additional file 5: Figure S5. The accumulation of misfolded SOD1 precedes glia activation. Representative immunofluorescence staining of Iba1, GFAP (red) or misfolded SOD1 (B8H10, green) proteins in the lumbar spinal cord sections of WT and mutant SOD1^{G93A} mice during the course of the disease (3, 6 and 17 weeks). Scale bars = 100 μm. The mean ± SEM fluorescence intensity expressed by arbitrary units is presented in the bar graph (*n* = 4 mice for each time point, five fields were analyzed for each mouse). ****p* < 0.001—compared to control mice (WT). n.s. = non significant.

Additional file 6: Figure S6. Detection of cPLA₂α and TNFα in motor neurons expressing hSOD1^{WT} or mutant hSOD1^{G93A}. The Pearson coefficient correlation between cPLA₂α and misfolded SOD1 (*r* = 0.87) and between cPLA₂α and TNFα (*r* = 0.96) in motor neurons expressing mutant SOD1^{G93A}. Representative results of fluorescence intensity of immunostaining presented in Figs. 3C and 6C is expressed in arbitrary units.

Additional file 7: Figure S7. Elevated TNFα levels in supernatant of NSC34 cells expressing SOD1^{G93A}. The levels of TNFα in the supernatants of NSC34 cells transfected with human SOD1^{WT} or mutant SOD1^{G93A} plasmids (as described in Fig. 6B) detected by ELISA. The bar graph is the mean ± SE of three experiments. Significance compared to control ****p* < 0.001, n.s. non-significant.

Acknowledgements

We thank Miss Dorothy Polayes, Florida, USA, for her a generous donation to support research on Degenerative Diseases at Ben-Gurion University of the Negev. We thank Ms. Shir Barel for helping with the purification of the plasmids used for transfection.

Authors' contributions

YME searched the literature, designed and carried out experiments, researched the data, prepared Figures. YS carried out experiments, researched the data, prepared Figures. LA carried out experiments, researched the data. NH and AI participated in the design of the study and guided some methodologies. RL designed the study, directed the study and wrote the manuscript. All authors read and approved the final manuscript.

Funding

This research was supported by a generous donation from Miss Dorothy Polayes, Florida, USA, during 2016–2019.

Availability of data and materials

There is no data, software, databases, and application/tool available apart from the reported in the present study. All data generated or analyzed during this study are included in this published article are provided in the manuscript and its Additional files.

Declarations

Ethics approval and consent to participate

The study was approved by Ben-Gurion University Institutional Animal Care and Use Committee (IL-40-07-2016) and was conducted according to the Israeli Animal Welfare Act following the guidelines of the Guide for Care and Use of Laboratory Animal (National Research Council, 1996).

Consent for publication

Not applicable.

Competing interests

The authors declare that they have no competing interests.

Author details

¹Immunology and Infectious Diseases Laboratory, Department of Clinical Biochemistry and Pharmacology, Faculty of Health Sciences, Ben-Gurion University of the Negev and Soroka University Medical Center, 84105 Beer Sheva, Israel. ²Department of Physiology and Cell Biology, Faculty of Health Sciences and The Zlotowski Center for Neuroscience, Ben-Gurion University of the Negev, Beer Sheva, Israel.

Received: 1 April 2021 Accepted: 17 November 2021

Published online: 25 November 2021

References

- Ince P, Highley J, Kirby J, Wharton S, Takahashi H, Strong M, Shaw P. Molecular pathology and genetic advances in amyotrophic lateral sclerosis: an emerging molecular pathway and the significance of glial pathology. *Acta Neuropathol.* 2011;122:657–71.
- Andersen P. Genetics of sporadic ALS. *Amyotroph Lateral Scler Other Motor Neuron Disord.* 2001;2:S37–41.
- Philips T, Robberecht W. Neuroinflammation in amyotrophic lateral sclerosis: role of glial activation in motor neuron disease. *Lancet Neurol.* 2011;10:253–63.
- Yoshihara T, Ishigaki S, Yamamoto M, Liang Y, Niwa J, Takeuchi H, Doyu M, Sobue G. Differential expression of inflammation- and apoptosis-related genes in spinal cords of a mutant SOD1 transgenic mouse model of familial amyotrophic lateral sclerosis. *J Neurochem.* 2002;80:158–67.
- Chiu I, Phatnani H, Kuligowski M, Tapia J, Carrasco M, Zhang M, Maniatis T, Carroll M. Activation of innate and humoral immunity in the peripheral nervous system of ALS transgenic mice. *Proc Natl Acad Sci U S A.* 2009;106:20960–5.
- Beers D, Henkel J, Xiao Q, Zhao W, Wang J, Yen A, Siklos L, McKercher S, Appel S. Wild-type microglia extend survival in PU.1 knockout mice with familial amyotrophic lateral sclerosis. *Proc Natl Acad Sci U S A.* 2006;103:16021–6.
- Nagai M, Re D, Nagata T, Chalazonitis A, Jessell T, Wichterle H, Przedborski S. Astrocytes expressing ALS-linked mutated SOD1 release factors selectively toxic to motor neurons. *Nat Neurosci.* 2007;10:615–22.

8. Kramer RM, Roberts EF, Manetta J, Putnam JE. The Ca²⁺(+)-sensitive cytosolic phospholipase A2 is a 100-kDa protein in human monoblast U937 cells. *J Biol Chem*. 1991;266:5268–72.
9. Clark JD, Milona N, Knopf JL. Purification of a 110-kilodalton cytosolic phospholipase A2 from the human monocytic cell line U937. *Proc Natl Acad Sci USA*. 1990;87:7708–12.
10. Stephenson DT, Lemere CA, Selkoe DJ, Clemens JA. Cytosolic phospholipase A2 (cPLA2) immunoreactivity is elevated in Alzheimer's disease brain. *Neurobiol Dis*. 1996;3:51–63.
11. Clemens JA, et al. Reactive glia express cytosolic phospholipase A2 after transient global forebrain ischemia in the rat. *Stroke*. 1996;27:527–35.
12. Stephenson D, Rash K, Smalstig B, Roberts E, Johnstone E, Sharp J, Panetta J, Little S, Kramer R, Clemens J. Cytosolic phospholipase A2 is induced in reactive glia following different forms of neurodegeneration. *Glia*. 1999;27:110–28.
13. Shibata N, Kakita A, Takahashi H, Ihara Y, Nobukuni K, Fujimura H, Sakoda S, Kobayashi M. Increased expression and activation of cytosolic phospholipase A2 in the spinal cord of patients with sporadic amyotrophic lateral sclerosis. *Acta Neuropathol*. 2010;119:345–54.
14. Kiaei M, Kipiani K, Petri S, Choi D, Chen J, Calingasan N, Beal M. Integrative role of cPLA with COX-2 and the effect of non-steroidal anti-inflammatory drugs in a transgenic mouse model of amyotrophic lateral sclerosis. *J Neurochem*. 2005;93:403–11.
15. Solomonov Y, Hadad N, Levy R. Reduction of cytosolic phospholipase A2alpha upregulation delays the onset of symptoms in SOD1^{G93A} mouse model of amyotrophic lateral sclerosis. *J Neuroinflammation*. 2016;13:134.
16. Johnston JA, Dalton MJ, Gurney ME, Kopito RR. Formation of high molecular weight complexes of mutant Cu, Zn-superoxide dismutase in a mouse model for familial amyotrophic lateral sclerosis. *Proc Natl Acad Sci USA*. 2000;97:12571–6.
17. Baron R, Babcock AA, Nemirovsky A, Finsen B, Monsonego A. Accelerated microglial pathology is associated with Abeta plaques in mouse models of Alzheimer's disease. *Aging Cell*. 2014;13:584–95.
18. Shmelzer Z, Haddad N, Admon E, Pessach I, Leto TL, Eitan-Hazan Z, Hershinkel M, Levy R. Unique targeting of cytosolic phospholipase A2 to plasma membranes mediated by the NADPH oxidase in phagocytes. *J Cell Biol*. 2003;162:683–92.
19. Leyton-Jaimes MF, Benaim C, Abu-Hamad S, Kahn J, Guetta A, Bucala R, Israelson A. Endogenous macrophage migration inhibitory factor reduces the accumulation and toxicity of misfolded SOD1 in a mouse model of ALS. *Proc Natl Acad Sci USA*. 2016;113:10198–203.
20. Royo NC, Vandenberghe LH, Ma JY, Hauspurg A, Yu L, Maronski M, Johnston J, Dichter MA, Wilson JM, Watson DJ. Specific AAV serotypes stably transduce primary hippocampal and cortical cultures with high efficiency and low toxicity. *Brain Res*. 2008;1190:15–22.
21. Maier O, Bohm J, Dahm M, Bruck S, Beyer C, Johann S. Differentiated NSC-34 motoneuron-like cells as experimental model for cholinergic neurodegeneration. *Neurochem Int*. 2013;62:1029–38.
22. Shvil N, Banerjee V, Zoltsman G, Shani T, Kahn J, Abu-Hamad S, Papo N, Engel S, Bernhagen J, Israelson A. MIF inhibits the formation and toxicity of misfolded SOD1 amyloid aggregates: implications for familial ALS. *Cell Death Dis*. 2018;9:107.
23. Hadad N, Tual L, Elgazar-Carmom V, Levy R, Levy R. Endothelial ICAM-1 protein induction is regulated by cytosolic phospholipase A2alpha via both NF-kappaB and CREB transcription factors. *J Immunol*. 2011;186:1816–27.
24. Yang CM, Lee IT, Chi PL, Cheng SE, Hsiao LD, Hsu CK. TNF-alpha induces cytosolic phospholipase A2 expression via Jak2/PDGFR-dependent Elk-1/p300 activation in human lung epithelial cells. *Am J Physiol Lung Cell Mol Physiol*. 2014;306:L543–551.
25. Liu NK, Deng LX, Zhang YP, Lu QB, Wang XF, Hu JG, Oakes E, Bonventre JV, Shields CB, Xu XM. Cytosolic phospholipase A2 protein as a novel therapeutic target for spinal cord injury. *Ann Neurol*. 2014;75:644–58.
26. Liu NK, Xu XM. Phospholipase A2 and its molecular mechanism after spinal cord injury. *Mol Neurobiol*. 2010;41:197–205.
27. Liu NK, Zhang YP, Han S, Pei J, Xu LY, Lu PH, Shields CB, Xu XM. Annexin A1 reduces inflammatory reaction and tissue damage through inhibition of phospholipase A2 activation in adult rats following spinal cord injury. *J Neuropathol Exp Neurol*. 2007;66:932–43.
28. Liu NK, Zhang YP, Tittsworth WL, Jiang X, Han S, Lu PH, Shields CB, Xu XM. A novel role of phospholipase A2 in mediating spinal cord secondary injury. *Ann Neurol*. 2006;59:606–19.
29. Lucas KK, Svensson CI, Hua XY, Yaksh TL, Dennis EA. Spinal phospholipase A2 in inflammatory hyperalgesia: role of group IVA cPLA2. *Br J Pharmacol*. 2005;144:940–52.
30. Bonventre JV. Roles of phospholipases A2 in brain cell and tissue injury associated with ischemia and excitotoxicity. *J Lipid Mediat Cell Signal*. 1997;16:199–208.
31. Farooqui AA, Yang HC, Rosenberger TA, Horrocks LA. Phospholipase A2 and its role in brain tissue. *J Neurochem*. 1997;69:889–901.
32. Tittsworth WL, Liu NK, Xu XM. Role of secretory phospholipase a(2) in CNS inflammation: implications in traumatic spinal cord injury. *CNS Neurol Disord Drug Targets*. 2008;7:254–69.
33. Tortarolo M, Vallarola A, Lidonnicci D, Battaglia E, Gensano F, Spaltro G, Fior-daliso F, Corbelli A, Garetto S, Martini E, et al. Lack of TNF-alpha receptor type 2 protects motor neurons in a cellular model of amyotrophic lateral sclerosis and in mutant SOD1 mice but does not affect disease progression. *J Neurochem*. 2015;135:109–24.
34. Kazuki Ohuchi K, Tsuruma K, Masamitsu Shimazawa M, Junji Nakamura J, Hideaki HH. The novel cPLA2 inhibitor AK106-001616 has a protective effect on SOD1^{G93A}-induced cell death in NSC34 murine motor neuron-like cell. *Pharmacol Pharmacy*. 2016;7:193–9.
35. Forsberg K, Jonsson PA, Andersen PM, Bergemalm D, Graffmo KS, Hultdin M, Jacobsson J, Rosquist R, Marklund SL, Brannstrom T. Novel antibodies reveal inclusions containing non-native SOD1 in sporadic ALS patients. *PLoS ONE*. 2010;5:e11552.
36. Ohyagi Y, Asahara H, Chui DH, Tsuruta Y, Sakae N, Miyoshi K, Yamada T, Kikuchi H, Taniwaki T, Murai H, et al. Intracellular Abeta42 activates p53 promoter: a pathway to neurodegeneration in Alzheimer's disease. *FASEB J*. 2005;19:255–7.
37. Bradley SV, Holland EC, Liu GY, Thomas D, Hyun TS, Ross TS. Huntingtin interacting protein 1 is a novel brain tumor marker that associates with epidermal growth factor receptor. *Cancer Res*. 2007;67:3609–15.
38. Ames HM, Bichakjian CK, Liu GY, Oravec-Wilson KI, Fullen DR, Verhaegen ME, Johnson TM, Dlugosz AA, Ross TS. Huntingtin-interacting protein 1: a Merkel cell carcinoma marker that interacts with c-Kit. *J Invest Dermatol*. 2011;131:2113–20.
39. Israelson A, Arbel N, Da Cruz S, Ilieva H, Yamanaka K, Shoshan-Barmatz V, Cleveland DW. Misfolded mutant SOD1 directly inhibits VDAC1 conductance in a mouse model of inherited ALS. *Neuron*. 2010;67:575–87.
40. Shteinfer-Kuzmine A, Argueti S, Gupta R, Shvil N, Abu-Hamad S, Gropper Y, Hoerber J, Magri A, Messina A, Kozlova EN, et al. A VDAC1-derived N-terminal peptide inhibits mutant SOD1-VDAC1 interactions and toxicity in the SOD1 model of ALS. *Front Cell Neurosci*. 2019;13:346.
41. Israelson A, Ditsworth D, Sun S, Song S, Liang J, Hruska-Plochan M, McAlonis-Downes M, Abu-Hamad S, Zoltsman G, Shani T, et al. Macrophage migration inhibitory factor as a chaperone inhibiting accumulation of misfolded SOD1. *Neuron*. 2015;86:218–32.
42. Maatkamp A, Vlug A, Haasdijk E, Troost D, French PJ, Jaarsma D. Decrease of Hsp25 protein expression precedes degeneration of motoneurons in ALS-SOD1 mice. *Eur J Neurosci*. 2004;20:14–28.
43. Kato S, Saeki Y, Aoki M, Nagai M, Ishigaki A, Itoyama Y, Kato M, Asayama K, Awaya A, Hirano A, Ohama E. Histological evidence of redox system breakdown caused by superoxide dismutase 1 (SOD1) aggregation is common to SOD1-mutated motor neurons in humans and animal models. *Acta Neuropathol*. 2004;107:149–58.
44. Pasinelli P, Belford ME, Lennon N, Bacskai BJ, Hyman BT, Trotti D, Brown RH Jr. Amyotrophic lateral sclerosis-associated SOD1 mutant proteins bind and aggregate with Bcl-2 in spinal cord mitochondria. *Neuron*. 2004;43:19–30.
45. Kolossov VL, Sivaguru M, Huff J, Luby K, Kanakaraju K, Gaskins HR. Airyscan super-resolution microscopy of mitochondrial morphology and dynamics in living tumor cells. *Microsc Res Tech*. 2018;81:115–28.
46. Sieben C, Douglass KM, Guichard P, Manley S. Super-resolution microscopy to decipher multi-molecular assemblies. *Curr Opin Struct Biol*. 2018;49:169–76.
47. Hazan-Halevy I, Seger R, Levy R. The requirement of both extracellular regulated kinase and p38 mitogen-activated protein kinase for stimulation of cytosolic phospholipase A(2) activity by either FcgammaRIIA or

- FcγRIIIB in human neutrophils. A possible role for Pyk2 but not for the Grb2-Sos-Shc complex. *J Biol Chem*. 2000;275:12416–23.
48. Szaingurten-Solodkin I, Hadad N, Levy R. Regulatory role of cytosolic phospholipase A2α in NADPH oxidase activity and in inducible nitric oxide synthase induction by aggregated Aβ1-42 in microglia. *Glia*. 2009;57:1727–40.
 49. Sagy-Bross C, Hadad N, Levy R. Cytosolic phospholipase Alpha upregulation mediates apoptotic neuronal death induced by aggregated amyloid-beta peptide. *Neurochem Int*. 2013;63:541–50.
 50. Sagy-Bross C, Kasianov K, Solomonov Y, Braiman A, Friedman A, Hadad N, Levy R. The role of cytosolic phospholipase A alpha in amyloid precursor protein induction by amyloid beta: implication for neurodegeneration. *J Neurochem*. 2014;132:559–71.
 51. Lee CW, Lin CC, Lee IT, Lee HC, Yang CM. Activation and induction of cytosolic phospholipase A2 by TNF-α mediated through Nox2, MAPKs, NF-κB, and p300 in human tracheal smooth muscle cells. *J Cell Physiol*. 2011;226:2103–14.
 52. Malada-Edelstein YF, Hadad N, Levy R. Regulatory role of cytosolic phospholipase A2 alpha in the induction of CD40 in microglia. *J Neuroinflammation*. 2017;14:33–59.
 53. Kaneko M, Stellwagen D, Malenka RC, Stryker MP. Tumor necrosis factor-α mediates one component of competitive, experience-dependent plasticity in developing visual cortex. *Neuron*. 2008;58:673–80.
 54. Yee AX, Hsu YT, Chen L. A metaplasticity view of the interaction between homeostatic and Hebbian plasticity. *Philos Trans R Soc Lond B Biol Sci* 2017; 372.
 55. Jung YJ, Tweedie D, Scerba MT, Greig NH. Neuroinflammation as a factor of neurodegenerative disease: thalidomide analogs as treatments. *Front Cell Dev Biol*. 2019;7:313.
 56. Tartaglia LA, Goeddel DV. Two TNF receptors. *Immunol Today*. 1992;13:151–3.
 57. Tewari M, Dixit VM. Recent advances in tumor necrosis factor and CD40 signaling. *Curr Opin Genet Dev*. 1996;6:39–44.
 58. Venters HD, Dantzer R, Kelley KW. A new concept in neurodegeneration: TNFα is a silencer of survival signals. *Trends Neurosci*. 2000;23:175–80.
 59. Poloni M, Facchetti D, Mai R, Micheli A, Agnoletti L, Francolini G, Mora G, Camana C, Mazzini L, Bachetti T. Circulating levels of tumour necrosis factor-α and its soluble receptors are increased in the blood of patients with amyotrophic lateral sclerosis. *Neurosci Lett*. 2000;287:211–4.
 60. Elliott JL. Cytokine upregulation in a murine model of familial amyotrophic lateral sclerosis. *Brain Res Mol Brain Res*. 2001;95:172–8.
 61. Hensley K, Fedynyshyn J, Ferrell S, Floyd RA, Gordon B, Grammas P, Hamdheydari L, Mhatre M, Mou S, Pye QN, et al. Message and protein-level elevation of tumor necrosis factor alpha (TNF alpha) and TNF alpha-modulating cytokines in spinal cords of the G93A-SOD1 mouse model for amyotrophic lateral sclerosis. *Neurobiol Dis*. 2003;14:74–80.
 62. Hensley K, Floyd RA, Gordon B, Mou S, Pye QN, Stewart C, West M, Williamson K. Temporal patterns of cytokine and apoptosis-related gene expression in spinal cords of the G93A-SOD1 mouse model of amyotrophic lateral sclerosis. *J Neurochem*. 2002;82:365–74.
 63. Jayachandran A, Mertens B, McKissick EA, Mitchell CS. Type I vs. type II cytokine levels as a function of SOD1 G93A mouse amyotrophic lateral sclerosis disease progression. *Front Cell Neurosci*. 2015;9:462–71.
 64. Welser-Alves JV, Milner R. Microglia are the major source of TNF-α and TGF-β1 in postnatal glial cultures; regulation by cytokines, lipopolysaccharide, and vitronectin. *Neurochem Int*. 2013;63:47–53.
 65. Kiaei M, Petri S, Kipiani K, Gardian G, Choi DK, Chen J, Calingasan NY, Schafer P, Muller GW, Stewart C, et al. Thalidomide and lenalidomide extend survival in a transgenic mouse model of amyotrophic lateral sclerosis. *J Neurosci*. 2006;26:2467–73.
 66. Pinkoski MJ, Droin NM, Green DR. Tumor necrosis factor alpha upregulates non-lymphoid Fas-ligand following superantigen-induced peripheral lymphocyte activation. *J Biol Chem*. 2002;277:42380–5.
 67. Veglianesi P, Lo Coco D, Bao Cutrona M, Magnoni R, Pennacchini D, Pozzi B, Gowing G, Julien JP, Tortarolo M, Bendotti C. Activation of the p38MAPK cascade is associated with upregulation of TNF alpha receptors in the spinal motor neurons of mouse models of familial ALS. *Mol Cell Neurosci*. 2006;31:218–31.
 68. Tortarolo M, Veglianesi P, Calvaresi N, Botturi A, Rossi C, Giorgini A, Migheli A, Bendotti C. Persistent activation of p38 mitogen-activated protein kinase in a mouse model of familial amyotrophic lateral sclerosis correlates with disease progression. *Mol Cell Neurosci*. 2003;23:180–92.
 69. Boillee S, Yamanaka K, Lobsiger C, Copeland N, Jenkins N, Kassiotis G, Kollias G, Cleveland D. Onset and progression in inherited ALS determined by motor neurons and microglia. *Science*. 2006;312:1389–92.
 70. Jaarsma D, Teuling E, Haasdijk ED, De Zeeuw CI, Hoogenraad CC. Neuron-specific expression of mutant superoxide dismutase is sufficient to induce amyotrophic lateral sclerosis in transgenic mice. *J Neurosci*. 2008;28:2075–88.
 71. Boillee S, Vande Velde C, Cleveland DW. ALS: a disease of motor neurons and their nonneuronal neighbors. *Neuron*. 2006;52:39–59.
 72. Clement AM, Nguyen MD, Roberts EA, Garcia ML, Boillee S, Rule M, McMahon AP, Doucette W, Siwek D, Ferrante RJ, et al. Wild-type nonneuronal cells extend survival of SOD1 mutant motor neurons in ALS mice. *Science*. 2003;302:113–7.
 73. Yamanaka K, Chun SJ, Boillee S, Fujimori-Tonou N, Yamashita H, Gutmann DH, Takahashi R, Misawa H, Cleveland DW. Astrocytes as determinants of disease progression in inherited amyotrophic lateral sclerosis. *Nat Neurosci*. 2008;11:251–3.

Publisher's Note

Springer Nature remains neutral with regard to jurisdictional claims in published maps and institutional affiliations.

Ready to submit your research? Choose BMC and benefit from:

- fast, convenient online submission
- thorough peer review by experienced researchers in your field
- rapid publication on acceptance
- support for research data, including large and complex data types
- gold Open Access which fosters wider collaboration and increased citations
- maximum visibility for your research: over 100M website views per year

At BMC, research is always in progress.

Learn more biomedcentral.com/submissions

